TRITIUM IN SUPERCONDUTCORS
V. SANDU

Outlines

I. Motivation

II. Tritium in Metals

III. Tritium in Type I Superconductors: Tantalum

IV. Tritium in Low Temperature Type II Superconductors: Niobium

V. Tritium in MgB_2

Magurele: the pole of physics research in Romania: Physics Tetragon

National Institute of Materials Physics
"Horia Hulubei" National Institute of Nuclear Physics and Engineering
National Institute of Physics of Plasma, Laser and Radiation
National Institute of Earth Physics and Seismology
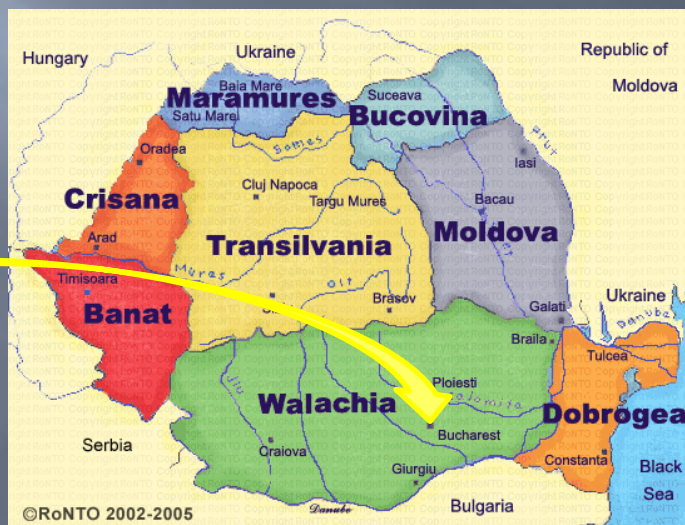
European laboratory
Extreme Light Infrastructure
THE ELI - nuclear physics facility

One of the three pillars of ELI, along with

1. the facilities dedicated to the study of secondary sources: Dolni Brezny, near Prague

2. attosecond pulses facility: Szeged

3. laser-based nuclear physics. It will generate radiation and particle beams with much higher energies, brilliances suited to studies of nuclear and fundamental processes.

- A very high intensity laser
Two 10 PW lasers are coherently added to get intensities of the order of 10^{23} - 10^{24} W/cm^2 and electrical fields of 10^{15} V/m;
- A very intense (10^{13} γ/s), brilliant γ beam, 0.1 % bandwidth, with E_v > 19 MeV, which is obtained by incoherent Compton back scattering of a laser light off a very brilliant, intense, classical electron beam (E_e > 700 MeV) produced by a warm linac.

National Institute of Materials Physics
The top research institute in Romania
The top institute in condensed matter physics in Romania

Multifunctional Materials and Structures

Magnetism and Superconductivity

Condensed Matter and Physics at Nanoscale

Optical Processes in Nanostructured Materials

Atomic Structures and Defects in Advanced Materials

Structural Characterization
Analytical Atomic Resolution Electron Microscope JEM-ARM200F (JEOL)
Scanning electron microscope Evo 50 XVP
Atomic Force Microscope AFM/PFM MFP-3D-SA (Asylum Research)
X-ray Diffractometers D8 ADVANCE type (BRUKER-AXS)

Spectro-ellipsometer WVASE 32 (Woollham)
UV-VIS-NIR Spectrophotometer, Lambda 90 (Perkin Elmer)
Spectrophotometer Fluorolog-3 FL3-22 (Horiba Jobin Yvon)
Scanning Near Field Photoluminescence Microspectrometer NSF- Jasco
Fluorescence Microscope AxioMat 1 (Engelmann Scientific)
Thermoluminescent Dosimeter TLD 3500 (Harshaw)
FT Raman Spectrophotometer RFS 100/S (Bruker)
FTIR Spectrophotometer Vertex 70 (Bruker)
FTIR Spectrometer SPECTRUM BX II (Perkin Elmer)
FTIR Imaging Microscope (Perkin Elmer)
Multiview 4000 SNOM (NANONICS)

Experimental Cluster for Surface and Interface Science:
  - The MBE (Molecular Beam Epitaxy) Chamber;
  - The STM (Scanning Tunneling Microscope) Chamber;
  - The Spin- and Angle-resolved Photoelectron Spectroscopy (SARPES).
Low energy and Photoelectron Electron Microscope LEEM-PEEM (Specs)
Ultra High Vacuum System for XPS/UPS/AES (Specs)

Network Analyzer E8361A PNA (Agilent)
PPMS & MPMS SQUID (Quantum Design)
Pulsed Terrahertz Time-Domain Spectrometer IRS 2000 Pro (Aispec)
Thermogravimetric/Differential Thermal Analysis (TG/DTA/DSC)
Magnetic Circular Dichroism Spectrometer (Jasco)
Broadband Dielectric Spectrometer (Novocontrol)
Surface Area and Porosimetry Analyzer ASAP 2020 (Micromeritics)

Fabrication facilities

Material processsing

- Hot-Press Sintering (MRF Inc.)
- Microwave Sintering (LINN)
- Spark Plasma Sintering (FCT)
- Melt spinner equipment (Buehler)
- Film evaporation system for organic materials (Lesker) (Engelmann Scientific)
- Multilayer Langmuir -Blodgett system KSV 5003
- Langmuir - Blodgett instrument KSV 2000 System 2
- Vacuum Deposition equipment with turbo-molecular pump
- Spin-coater deposition equipment

Nanofabrication of Materials

- Scanning Electron Microscope Lyra 3XMU with Focused Ion Beam SEM-FIB sample preparation system (Tescan) with EBSD and EDS analysis systems (Bruker)
- Scanning Electron Microscope S-3400 N (Hitachi) with Quantum Elphy nanolithography System and Laser Interferometer Ultra Precision Positioning Strage (Raith)
- Photolithography Mask Aligner EVG 620 NT with Nanoimprint Litography (EV Group)
- Pulsed Laser Deposition (PLD) Workstation for thin layer deposition, fit with in-situ Reflection High Energy Electron
- Diffraction (RHEED) analysis system (Surface)
- Magnetron Sputtering Equipment (Surrey NanoSystems Ltd.) with in-situ surface analysis techniques : AES, LEED (Omicron)

Class ISO 1000 and 100 Clean room Assembly

I. Motivation

Fusion reactions in fusion plants

1. D-T fuel cycle $\quad {}^2_1 D + {}^3_1 T \longrightarrow {}^4_2 H + {}^1_0 n$ requires the breeding of tritium from Li:

$$ {}^1_0 n + {}^6_3 Li \longrightarrow {}^3_1 T + {}^4_2 He $$
$$ {}^1_0 n + {}^7_3 Li \longrightarrow {}^3_1 T + {}^4_2 He + {}^1_0 n $$

2. D-D fuel cycle $\quad {}^2_1 D + {}^2_1 D \longrightarrow {}^3_1 T + {}^1_1 H$

$$ {}^2_1 D + {}^2_1 D \longrightarrow {}^3_2 He + {}^1_0 n $$
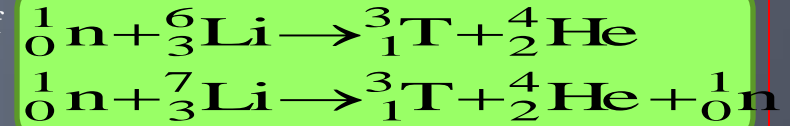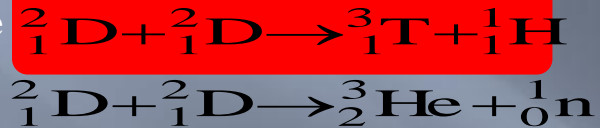
Problems: a) Handling of Tritium (difficult to contain)
       b) high neutron flux

3. D-³He fuel cycle $\quad {}^2_1 D + {}^3_2 He \longrightarrow {}^4_2 He + {}^1_1 p$

4. p-¹¹B fuel cycle $\quad {}^1_1 H + {}^{11}_5 B \longrightarrow 3\, {}^4_2 He$

Outer Intercoil Structure — Vacuum Vessel — Toroidal Field Coil — Central Solenoid — Cryostat — Poloidal Field Coil — Divertor — Port Plug (Ion Cyclotron System) — Machine Gravity Supports — Blanket Module — Torus Cryopump
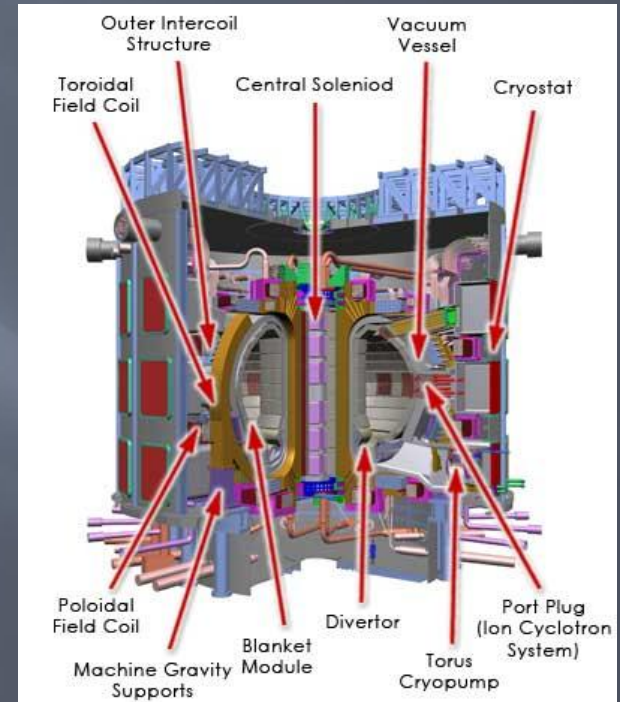
II.1. Hydrogen and isotopes

1. Impinge the surface
2. Dissociate
3. Diffuses through surface to the bulk
   - low density of H → α-phase
   - high density of H → ordering into **hydrides**
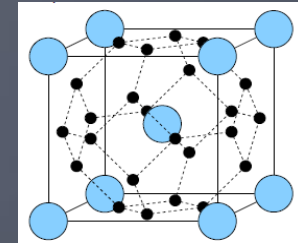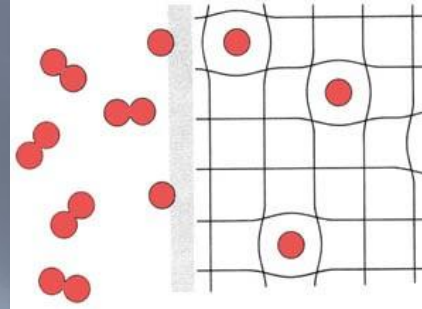
1. H has small size → enters interstitially
2. Prefers a) sites with tetrahedral interstitial sites (TIS) in BCC metals (dissolved H)
          b) extraordinary sites associated with crystal defects (trapped H)
3. Expands the host lattice
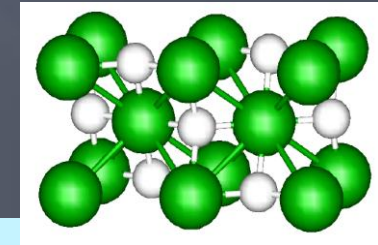
•2 H atoms tend to pair up at two neighboring TIS along the 110 directions
•The equilibrium distance of the H-H pair is 2.22 Å >> H_2 bond length of 0.75 Å. Not H_2 (yet)
•The H-embedding energy decreases monotonically with decreasing electron density until reaching a minimum at the optimal density of $n \approx 0.018$ e/Å^3 << $n_{metal} \Rightarrow$ vacancies are preferred.

Self trapping: host atoms relax from their equilibrium position this destroys the periodicity of the lattice
          -Hydrogen is trapped by its own distortion field
          -The energy levels of hydrogen are brought out of resonance

$V(R)$
--- Fixed
— Relaxed
$[\bar{1}10]$
H
Cu
$[110]$
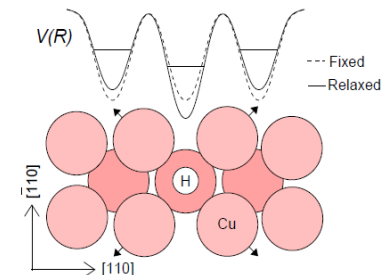
II.2. Diffusion

- Abnormally large diffusion rate in bcc metals: ~10^{-5}cm^2/s, typical for liquids

	H	^{2}H	^{3}H
Nb	5×10^{-5}	5.2×10^{-5}	4.5×10^{-5}
Ta	4.4×10^{-5}	4.6×10^{-5}	4.6×10^{-5}

J. Völkl, & G. Alefeld, Zeit. Physik. Chem NF 114 (1974)2 23
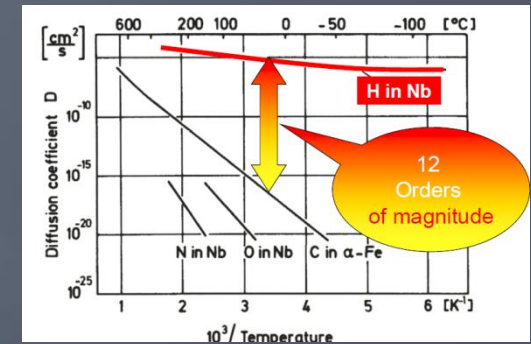
- Activation enthalpy ~0.1 eV, one order of magnitude smaller than for C, N, O.

- Jump rate ~10^{12}s^{-1}, only one order of magnitude lower than the highest frequency of the host lattice

- Temperature dependent mechanisms

    -very low T: delocalized interstitials (unless trapped by deffects)$\Rightarrow$ band state$\Rightarrow$ coherent tunneling (pseudo solid H in metallic cage)

    - $kT \ll \hbar\omega_m$: localized interstitials, phonons are necessary to equalize the energy levels of both sites $\Rightarrow$incoherent hopping of self trapped states

    - $kT < \hbar\omega_H$ thermally activated tunneling
    -$kT > \hbar\omega_H$: thermally activated jumps
    -$kT \gg V$: diffusion through collisions with phonons
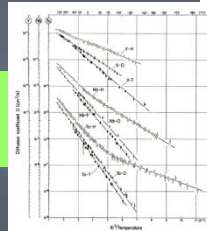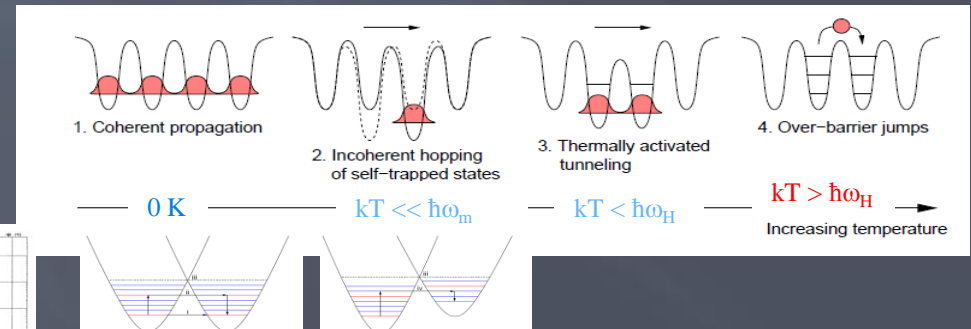
The rate of diffusion for H, D, T, in bulk BCC Nb & Ta

II.3. Effects of H and isotopes

(1) embrittlement,
(2) blistering,
(3) cracking from precipitation of internal hydrogen,
(4) hydrogen attack and cracking from hydride formation

1. Embrittlement:

   i) The absorbed hydrogen atom is too large to fit comfortably in the interstitial sites in the metal lattice and because of its mobility will migrate to extraordinary sites where the lattice is dilated: vacancies.

   H and vacancy are strongly attractive in metals
   the vacancy formation energy will be lowered by the presence of H in comparison with that in the intrinsic metal

   (111)
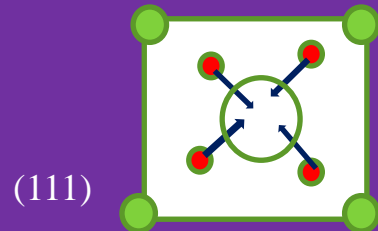
   Vacancies act as trapping centers which drive the H to segregate toward the vacancies

   A monovacancy can trap up to 10 H $\Rightarrow H_2 \Rightarrow$ bubble

   8 H   10 H
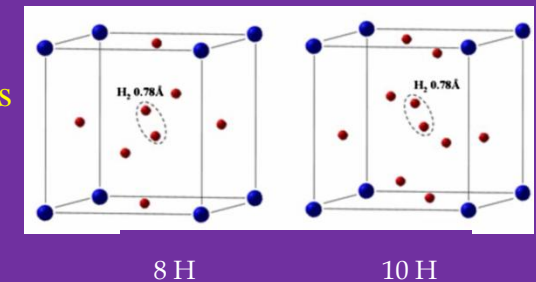
   ii) H loads will result in concentrated stresses that produce localized, macroscopic regions of lattice dilation.
   iii) H migrates to the region of lattice dilation increasing the hydrogen concentration in that region.
   iv) The crack nucleation and/or extension process relieves the stresses and associated lattice dilation
   v) H relocates to the newly dilated zone and the crack nucleation/propagation process will repeat

2. Blistering:

   i) the mobile, nascent hydrogen atoms collect at the extraordinary sites in the metal.

   ii) H recombines to form H_2

   iii) High pressure → plastic deformation → bump or blisters at surface

If the blister cannot rupture it can reversibly collapse!
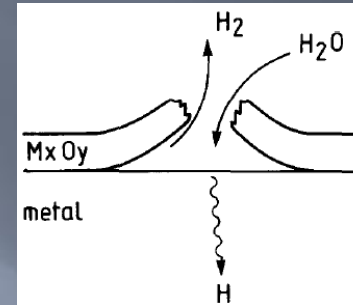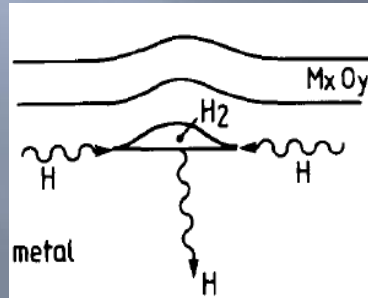
J B Condon & T Schober ,
J. Nucl. Mater. 207 (1992) 1
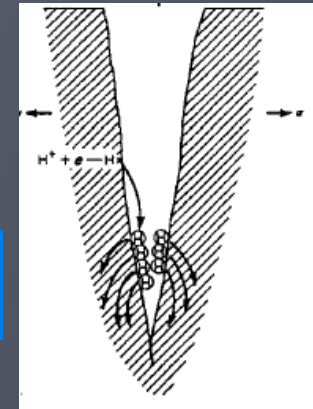
3. Cracks: *i*) precipitation of the internal H at the internal surfaces in voids increases the stress at the tip

   ii) the tip cannot blunt and the void extends which makes the pressure decrease

4. Hydrogen attack:

   i) H interacts with alloying or impurity elements in the microstructure to form an insoluble, generally gaseous, phase

$$4H + C \rightarrow CH_4$$

   ii) hydride formation

Tritium →radioactive decay $^3_1T \longrightarrow ^3_2He + ^{\ 1}_{-1}e + \tilde{\nu}$

Helium→ *i)*clustering
        ii) bubble formation

Repulsion between the conduction electrons and the occupied He core
No covalent bonding (He 1s level well below metal conduction band).

Relaxation caused by He is much larger → much larger self trapping energy
He self trapping energy similar to the vacancy-formation energy (W.D. Wilson et al., Phys. Rev. B 24 (1981) 5616)
He drives the vacancy generation → He trapped in vacancy → He clusters → Dislocations

Single He atoms may be caught by sinks and will not take part in further clustering in the matrix.
Sinks for helium atom:
            - lattice defects (dislocations, interstitial loops, vacancy clusters)
            - precipitates
            - grain boundaries

He is not lost but stored at the different sink sites ⇒ the sinks themselves may act as nucleation sites for further helium clustering.

II.5. SUPERCONDUCTIVITY

I.   Disorder
*   Anderson theorem: non-magnetic disorder should not significantly affect the critical temperature T_c as long as the system remains a metal (P.W. Anderson, *J. Phys. Chem. Solids* **11, 26 (1959))**.
*   Disorder might lead to the broadening of the DOS $\rightarrow$ changes in the electron-phonon coupling constant λ.

$$\xi \Rightarrow \sqrt{\xi_{BCS} l}$$

$$\lambda \Rightarrow \lambda\sqrt{\xi_{BCS}/l} \Rightarrow \kappa \sim \lambda/l \text{ possible conversion from Type I to Type II superconductor if } \kappa > 1/\sqrt{2}$$

II. Superconducting hydrides

Pd & alloys becomes superconductor T_c = 9 K in $PdH_{0.9}$ (T. Skoskiewic, phys . stat. sol. (a) 11, K123 (1972)).

T_c = 13.6 K in $Pd_{0.74}Au_{0.16}H$ (B Stritzer, Zeit. Phys268 (1974) 261)

T_c = 15.6 K in $Pd_{0.66}Ag_{0.33}H$ (B Stritzer, Zeit. Phys268 (1974) 261)

T_c = 16.6 K in $Pd_{0.55}Cu_{0.45}H$ ((B Stritzer, Zeit. Phys268 (1974) 261)

T_c = 11 K in PdD (B Stritzer & W. Buckel, Zeit. Phys257 (1972) 1)

Theorists still predict high temperature superconductivity in metallic hydrides (N W Ashcroft (Hydrogen Dominant Metallic Alloys: High Temperature Superconductors? Phys.Rev.Lett. 92 (2004) 187002)

II. 6. Experimental

Ta & Nb

- 2 hours tritiation in ampoules at 0.36 MBq/ml from a uranium bed storage system tritium
- 1 hour outgasing
- 8 hours annealing at 300 °C
- Immersion in ethylic alcohol
- 24 hours storage
- 2 hours drying at 90 °C

Tritium profile AMS
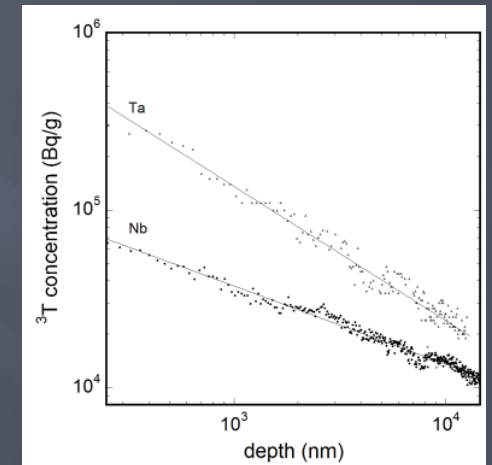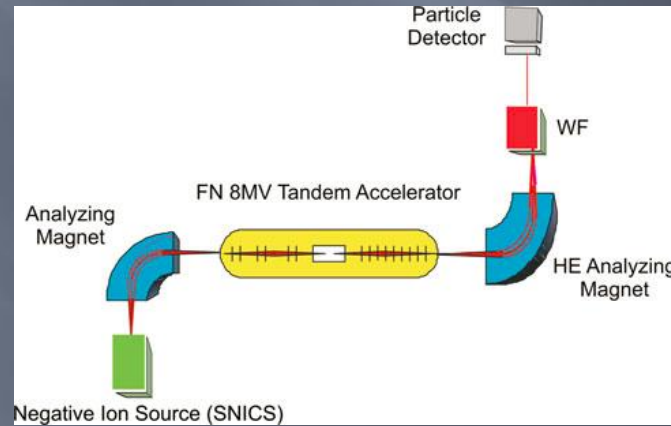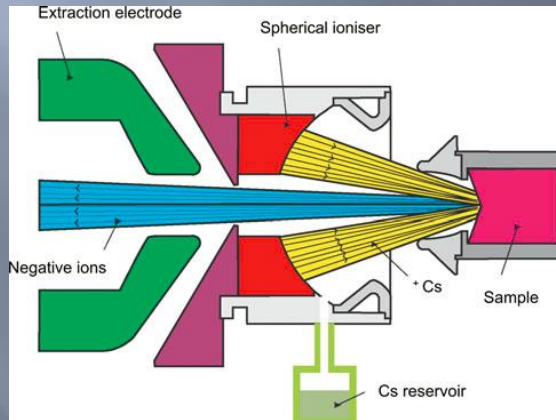
$$c(x) = c_s x^{-\alpha}$$

$\alpha_{Ta} = 0.76$
$\alpha_{Nb} = 0.44$

III. Tritium in Tantalum

Ta: Type I superconductor
T_c = 4.48 K
s-wave OP
κ = 0.42
B_c = 0.0780 T

XRD
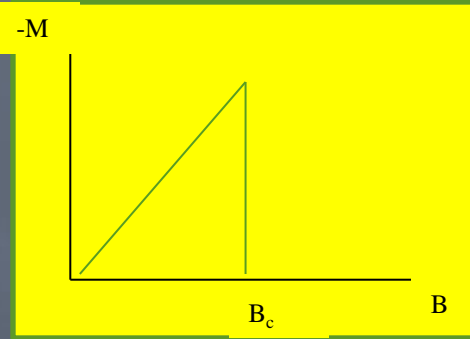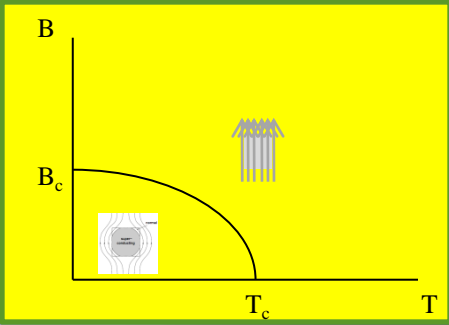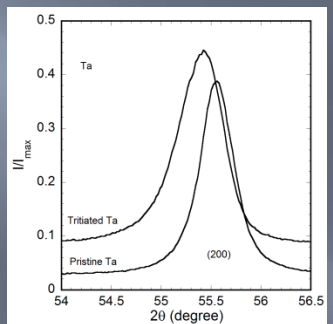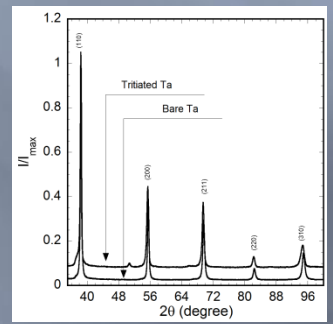
Lattice swelling

Critical temperature

Low H: type I phase transition with exaggerated supercooled state in the bare state.
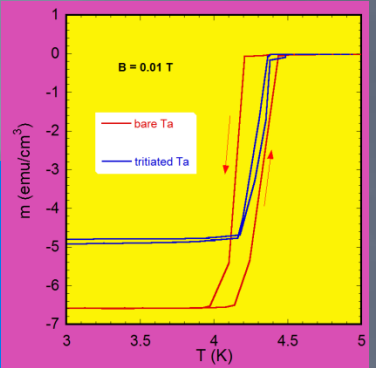
T_c(0.01 T) = 4.67 K
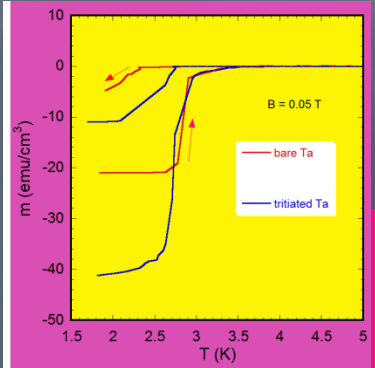
High H possible transition from type I to type II superconductivity.

T_c(0.05 T) = 4.49 K

III. 2. Magnetization

Hysteresis?!?
Possibilities:

    1. Ta driven in type II superconductor if a relatively small amount of interstitial defects are inserted.

    2. Topological pinning which results from the different topology of the intermediate state of the flux entry and flux exit state, respectively. Suprafroth state colapses into laminar state which are pinned by extrinsic sources
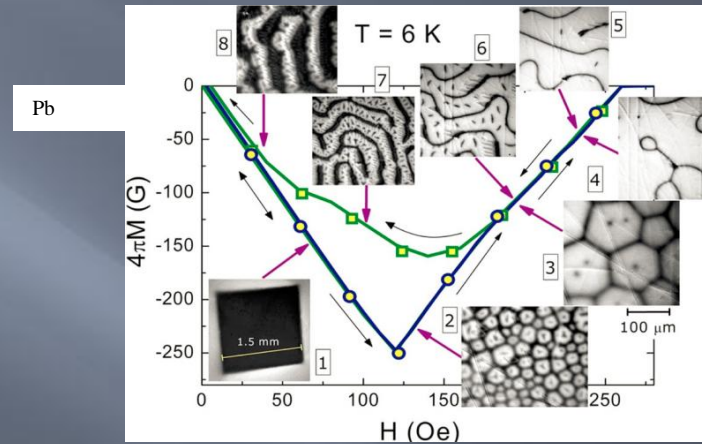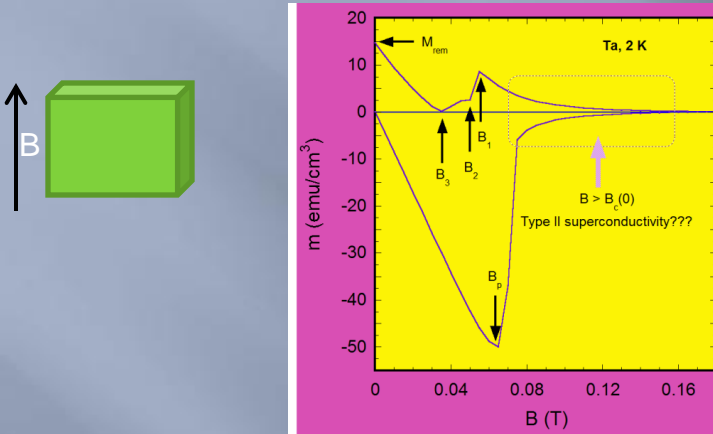
1-4 Flux entry
5-8 Flux exit

1. Pure Meissner screening
2, 3 Suprafroth state
5-8 laminar states

R. Prozorov et al., Phys. Rev B **72 (2005)** 212508

3. Pinning & Quantum tunneling of interfaces at low T
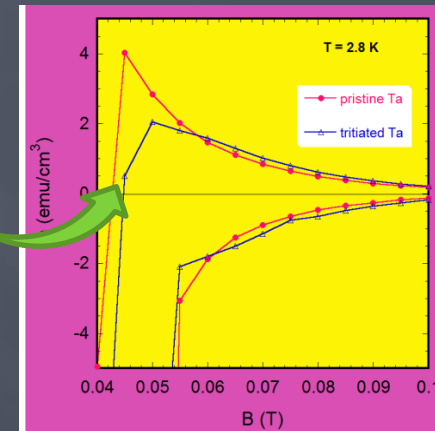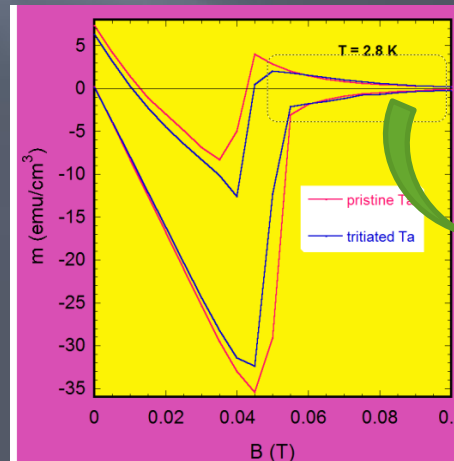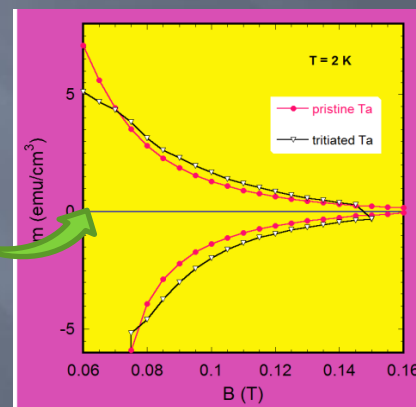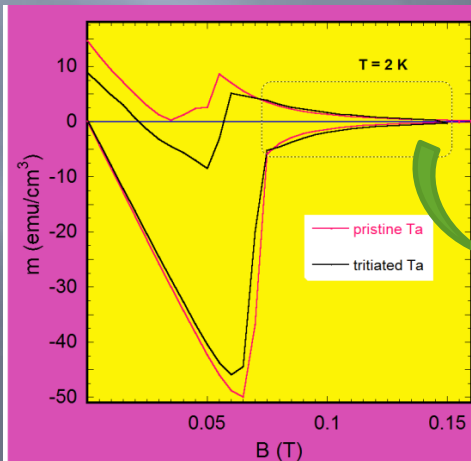
κ= 0.42 but $\kappa = \kappa_0 + 7.53\rho_0\gamma^{1/2}$ with ρ_0 = 13.6 R_{Tc}/R_{300} (BB Goodman, IBM J res Develop 6 (1962) 63

For $R_{Tc}/R_{300} > 0.04 \Rightarrow \kappa > 0.71 \Rightarrow$ Type II superconductor

IV. Tritium in Niobium

Nb: Type II superconductor
$T_c = 9.2$ K
s-wave OP
$\kappa = 1.69$
$B_c = 0.0780$ T

XRD
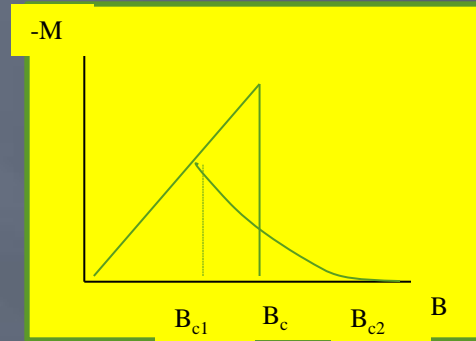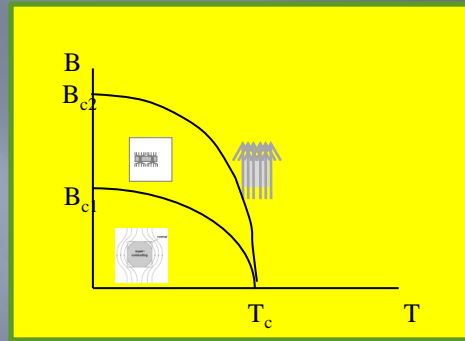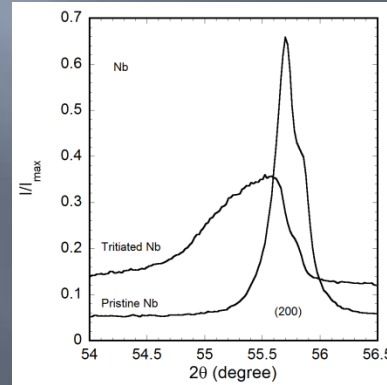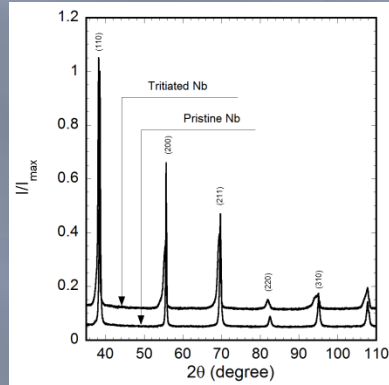
Lattice swelling

Critical temperature
Low H
$T_c = 9.3$ K $\Rightarrow$ 9.28 K
High H
$T_c = 6.6$K $\Rightarrow$ 5 K
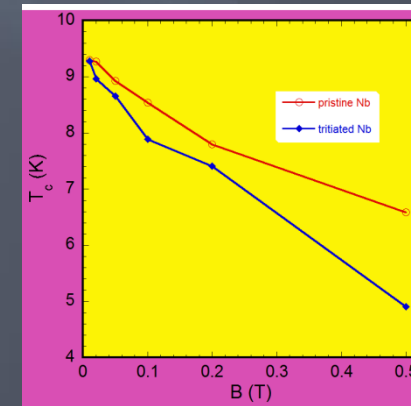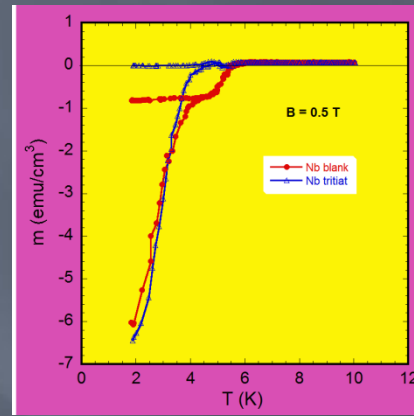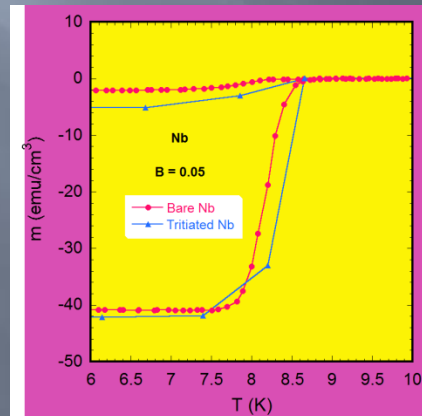
Magnetization
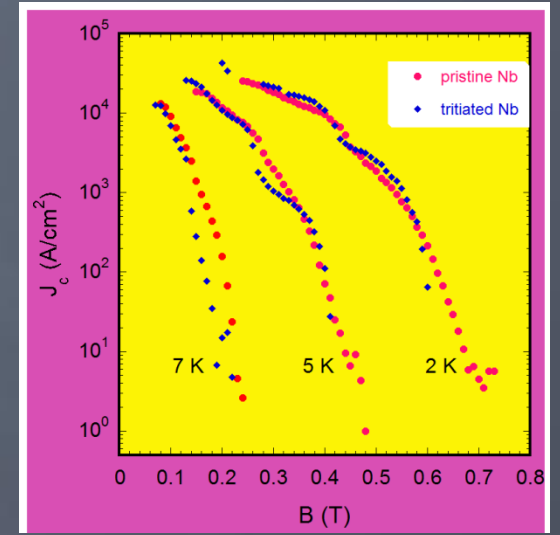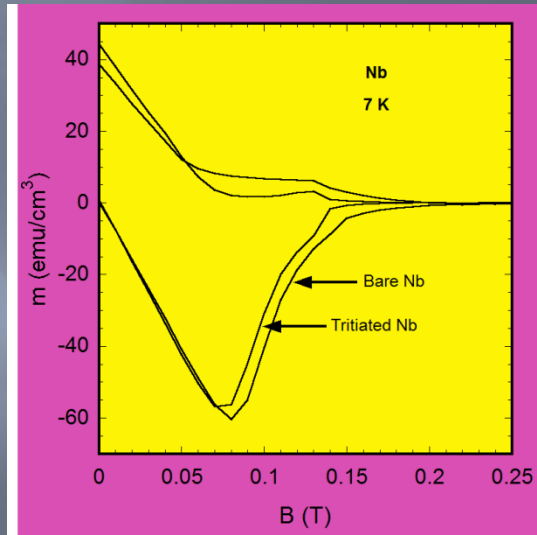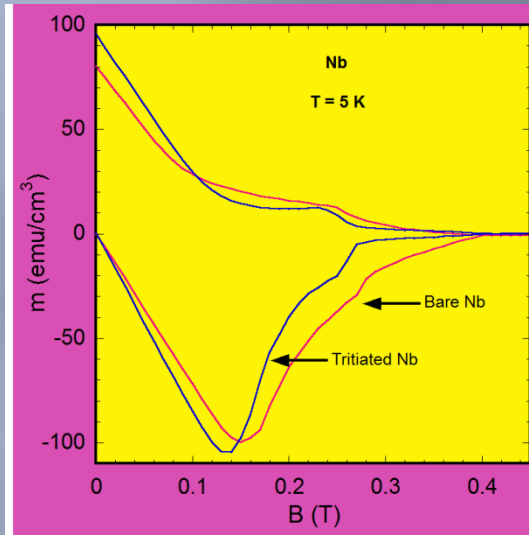
Nb is rather robust to titriation except high T (7 K)

V. MgB_2

- MgB_2 : phonon-mediated BCS-Eliashberg superconductor.

- Two superconducting gaps on disjoint Fermi sheets: π and σ

- The bands have : different symmetry and location in the **k**-space.

- Three distinct electron-phonon spectral functions: intra- and inter band pairing.

- T_c = 39 K

- Type II superconductor

- Self doping with holes

- B-planes associated to superconductivity

XRD

Why not hydrides?

H_2 dissociation energy 0.49-0.52 eV
Hydride formation requires a structural transition
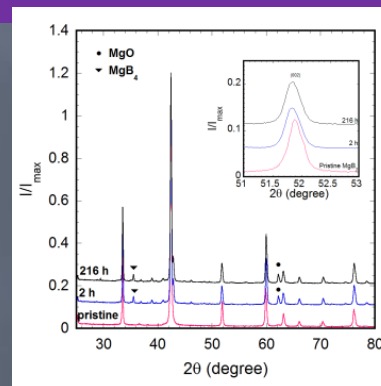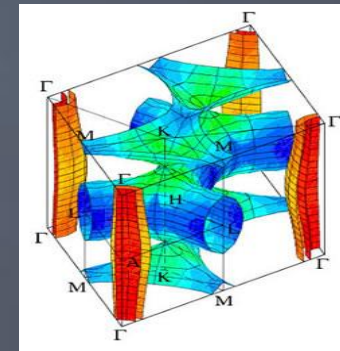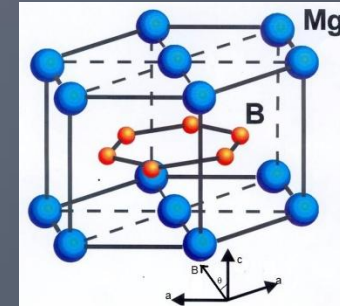
sample	a (Å)	c (Å)
Pristine	3.085	3.5201
2 h	3.083	3.5263
216 h	3.083	3.5264
Ideal	3.083	3.521

- *a* & *c* changes are beneficial for superconductivity.
 the increase of the Mg–B spacing shifts the dominant σ bands upwards with respect to the E_F, hence,
increases the number of holes despite a slight decrease in the π bands. (X Wan et al. Phys. Rev. B 65 (2001) 012502)
- increases the DOS $N(E_F) \Rightarrow$ the electron–phonon coupling constant λ .

Superconducting transition

Both tritiated samples show the same T_c
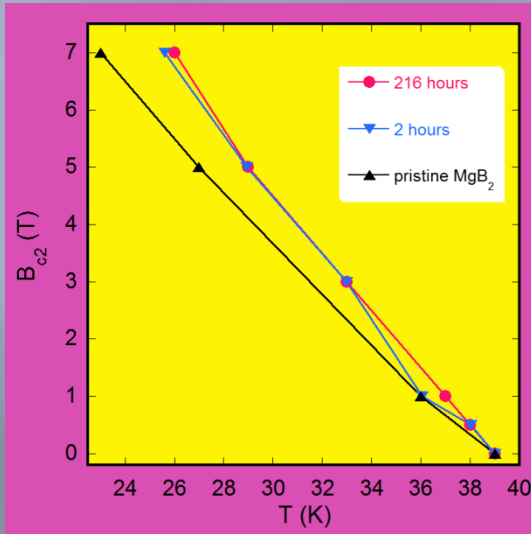
B_{c2} (T, 2 h) $\cong$ B_{c2} (T, 216h)
Limited solubility of tritium in MgB_2 crystallites
The rest goes to sinks
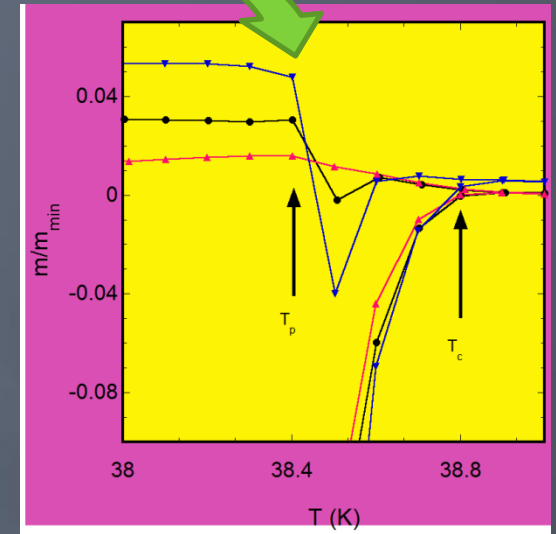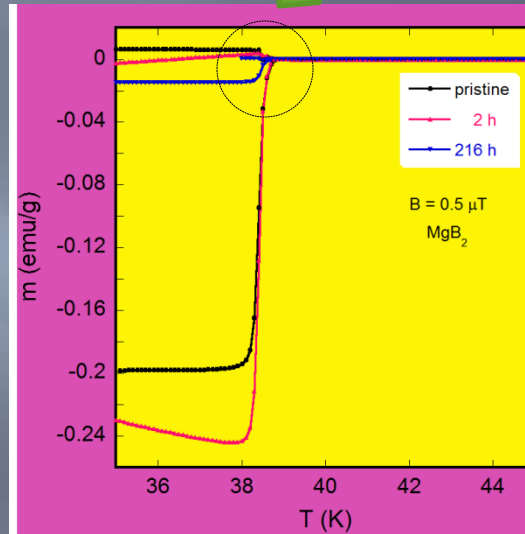
sample	T_c (K)		
	7 days	370 days	445 days
Pristine	38.8	38.8	38.8
2 h	39.1	38.8	38.5
216 h	39.1	38.8	38.5

Critical current density
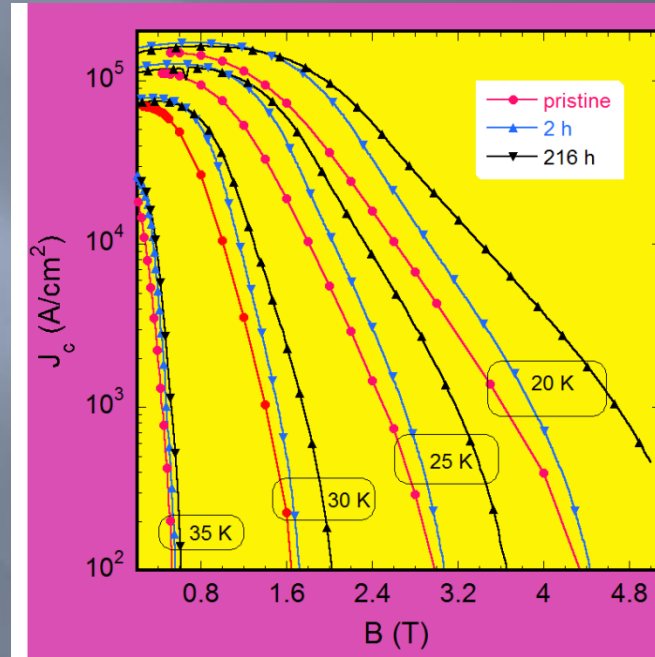
Scaled pinning force
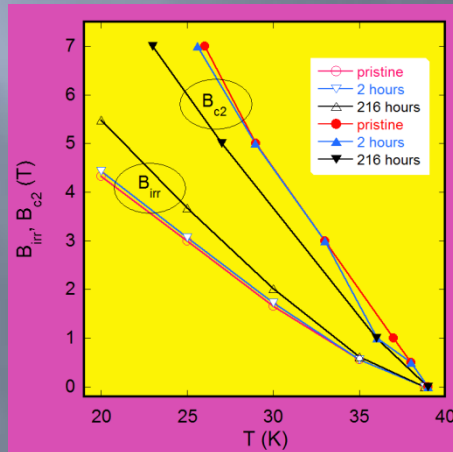
Long time irradiation $\Rightarrow$ defects valuable pinning centers
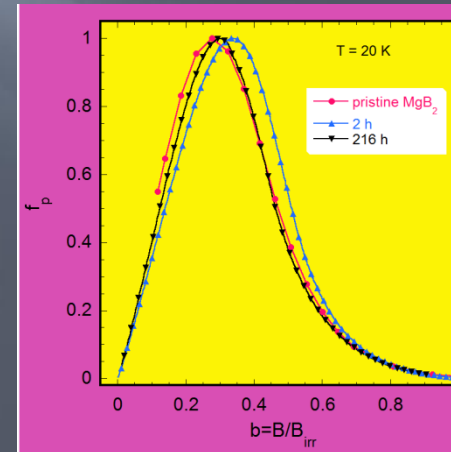
Similar mechanisms after pristine and long tritiated samples (grain boundaries)

Raman spectra

Phonon modes of Γ:

c axis	B_{1g}
	A_{2u}
in plane	E_{1u}
	E_{2g}

• The presence of the silent modes suggests that disorder has relaxed the selection rules to different degrees.
• The two peaks, LF and HF, are sampling the phonon density of state
• disorder expands the momentum space around the 0 point ($\mathbf{q}$ =0) of BZ that contributes to the Raman spectra $\Rightarrow$ additional broadening of the band
• the evolution of the LF and HF peaks indicative of the disorder generated by tritium uptake
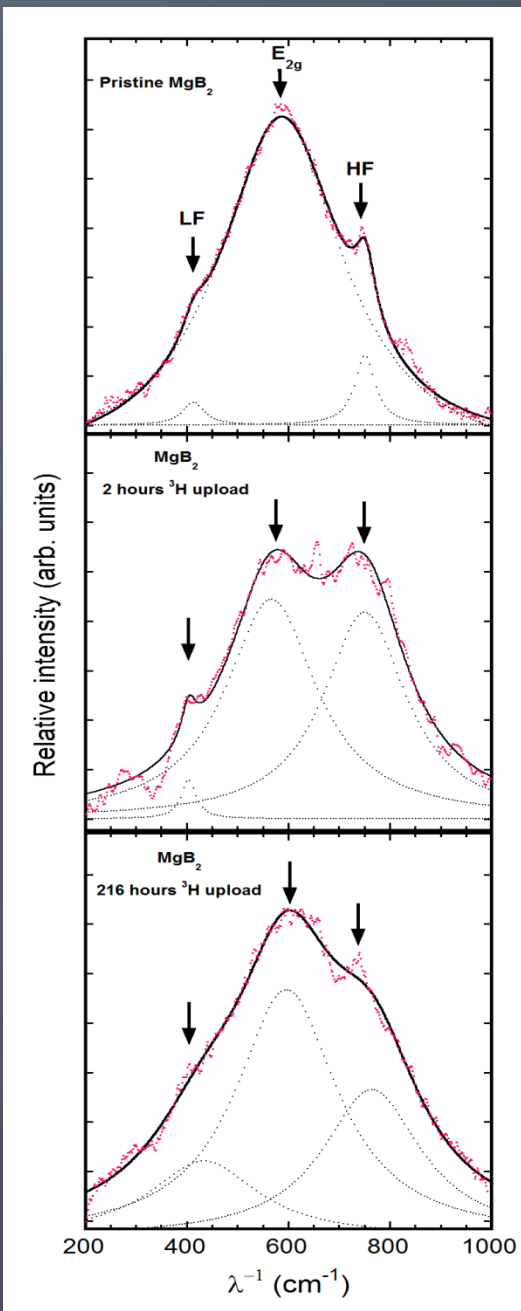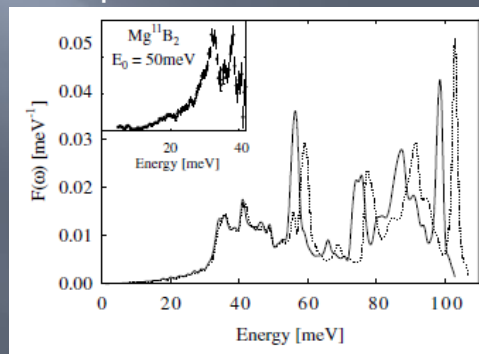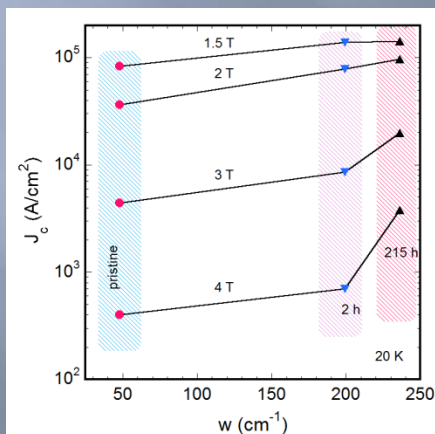
Raman characteristics of the pristine and tritiated samples

sample	Raman shift [cm^{-1}]			Raman FWHM [cm^{-1}]			λ	ω_0 [cm^{-1}]
	E_{2g}	LF	HF	w_{E2g}	w_{LF}	w_{HF}		
pristine	585	413	751	298	51	48	**3.11**	570
2 h	585	403	750	219	35	199	**2.43**	567
216 h	595	424	765	244	259	236	**2.46**	582

$$\lambda = \frac{w}{2\pi N(0)\omega^2} \ ???$$

In fact λ_{ij} i,j $=\sigma\pi$

Conclusions
1. Metallic, LTS, are slightly damaged by tritiation
2. MgB_2 is enhanced, at least at J_c
3. Remember that neutrons activation is high in fusion reactors
Life time of $^{94}Nb \sim 2 \times 10^4$ years
Life time of Mg, B $\sim 10^1$ years

Superconductivity group
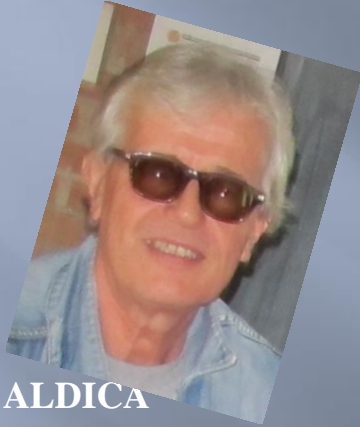
G. ALDICA
P. BADICA
M. BURDUSEL
I. IVAN
V. MIHALACHE
L. MIU
S. POPA
V. SANDU,

Thank you